LABORATORY OF BIOLOGICAL DIVERSITY

KIMORI Group

Specially Appointed Assistant Professor:
KIMORI, Yoshitaka

Image processing methods significantly contribute to visualization of biomedical targets acquired from a variety of imaging techniques, including: wide-field optical and electron microscopy, X-ray computed tomography, magnetic resonance imaging and mammography. Quantitative interpretation of the deluge of complicated biomedical images, however, poses many research challenges.

We have developed new computational methods based on mathematical morphology for quantitative image analysis. One of the most important purposes of image processing is to derive meaningful information, which is expressed as structural properties in images. Mathematical morphology is a nonlinear image processing method based on the set theory and is useful for the extraction of structural properties from an image. It can be used as a fundamental tool to analyze biomedical images and provides an objective, accurate alternative to manual image analysis.

Novel image analysis method based on mathematical morphology: quantifying morphological features of actin filaments in plant cells

Image processing is a crucial step in the quantification of biomedical structures from images. As such, it is fundamental to a wide range of biomedical imaging fields. Image processing derives structural features, which are then numerically quantified by image analysis. We can better evaluate complex shapes and detect subtle morphological changes in organisms by quantifying the shape properties. Therefore, we have developed a shape analysis method based on morphological image processing, and have applied it to image analysis of actin cytoskeletal filaments in root-hair cells of *Arabidopsis thaliana*. Actin cytoskeletal filaments have critical roles in various cellular processes in plant cells. To understand actin-dependent organelle motility, we analyzed the organization of actin filaments in the cells.

We measured three shape features of the actin filaments in wild-type and mutant (*root hair defective 3* (*rhd3*) mutant) plants. One feature i.e. thickness (*T*) was extracted from grayscale images; the others i.e. multi-orientation index (*MOI*) and complexity (*C*) were extracted from binary images. *T* of an actin filament was measured by a pattern spectrum which provides a distribution of filament thickness. *MOI* was measured by applying a series of opening operations to obtain the orientation distribution of the filament. *C* was computed from the fractal dimension of the filament network pattern. As the *MOI* and *C* quantify the complexity properties of the filament patterns in two-dimensional space, finally, these binary-based features were combined into a single feature called the binarized filament pattern feature (*BFPF*).

The *T* of the wild-type and mutant were 1.88 μm and 2.33 μm, respectively, and those were statistically different ($p < 0.001$). Also, *MOI* of the wild-type and *rhd3* mutant images were statistically different ($p < 0.01$), too. Finally, we calculated the *C*. The mean fractal dimension of the actin filament was significantly larger in the wild-type than in the *rhd3* mutant ($p < 0.001$). Furthermore, the mean *BFPF* (obtained by combining *MOI* and *C*) were again significantly differed between the two groups ($p < 0.001$). These results are summarized in a scatter plot of *BFPF* (*x*-axis) versus *T* (*y*-axis) (Left panel of Figure 1). First, we note that actin filaments are thicker in the *rhd3* mutant than in the wild-type. Second, both *MOI* and *C* are significantly larger in the wild-type filaments than in the *rhd3* mutant filaments. Overall, the filament patterns in two-dimensional space are more complex in the wild-type than in the *rhd3* mutant. The *rhd3* mutant data in the scatter plot are divisible into two classes (Class 1 and Class 2), distinguished by linear discriminant analysis (LDA). The right panel of Figure 1 shows three images selected from each class.

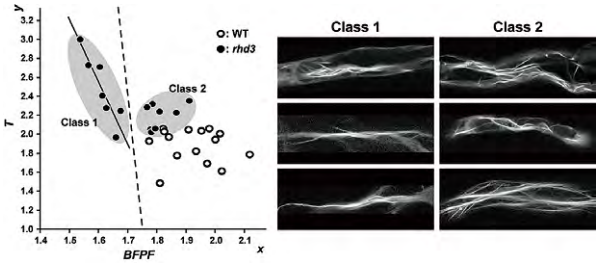

Figure 1. Left: Scatter plot of *BFPF* versus *T* for the actin filament of wild-type and the *rhd3* mutant. Data of the *rhd3* mutant is divided into two classes. Dashed line is classification boundary obtained by LDA. Solid line is boundary obtained by linear regression of the data in Class 1. Right: Actin filaments of the *rhd3* images belonging to each class.

Publication List:

〔Original paper〕

● Ohya, Y., Kimori, Y., Okada, H., and Ohnuki, S. (2015). Single-cell phenomics in budding yeast. Mol. Biol. Cell. *26*, 3920-3925.

〔Original papers (E-publication ahead of print)〕

● Kimori Y., Hikino K., Nishimura M. and Mano S. Quantifying Morphological Features of Actin Cytoskeletal Filaments in Plant Cells Based on Mathematical Morphology. J. Theor. Biol. 2015 Nov 10.
● Yasuda, T., Kimori, Y., Nagata, K., Igarashi, K., Watanabe-Asaka, T., Oda, S., and Mitani, H. Irradiation-injured brain tissues can self-renew in the absence of the pivotal tumor suppressor p53 in the medaka (*Oryzias latipes*) embryo. J. Radiat. Res. 2015 Sep 25.